Desalination and Water Treatment
www.deswater.com

doi: 10.1080/19443994.2015.1070756

57 (2016) 13807–13817
June

Taylor & Francis
Taylor & Francis Group

Ni(II) adsorption characteristics of commercial activated carbon from synthetic electroless plating solutions

Yennam Rajesh[a], Gummalla Namrata[b], Uppaluri Ramgopal[a,*]

[a]*Department of Chemical Engineering, Indian Institute of Technology Guwahati, Guwahati 781039, Assam, India, email: y.rajesh@iitg.ernet.in (Y. Rajesh), Tel. +91 361 2582260; Fax: +91 361 2582291; email: ramgopalu@iitg.ernet.in (U. Ramgopal)*

[b]*Department of Chemical Engineering-Plastics and Polymers, Birla Institute of Technology-Mesra, Jharkhand 835215, India, email: nmarata.gummalla@gmail.com*

Received 21 November 2014; Accepted 29 May 2015

ABSTRACT

Literature data with respect to Ni(II) adsorption from real process streams is scarce. The present work addresses the effect of solution complexity of electroless plating solution on the adsorption efficiency of commercial activated carbon adsorbent. Specific complexity refers to the inclusion of trisodium citrate in a basic medium. For all adsorption studies, the Ni(II) solution concentrations were varied from 50 to 500 mg/L in the pH range of 2–14. For these experiments, the adsorbent dosage was varied from 0.5 to 4 g/L. The optimum time or adsorption was evaluated prior to 120 min. The point of zero charge for the adsorbent was experimentally evaluated to be 10.23 and the optimum pH for Ni(II) adsorption was 10.55, which is in good agreement with the pH of the Ni(II) ELP solutions. The optimum adsorbent dosage was evaluated to be 4 g/L. The optimum percentage removal of Ni(II) was 44.54% for a maximum adsorption capacity of 17.75 mg/g. These values were significantly lower than those determined for aqueous solutions as reported in the literature. The Fourier transform infrared analysis indicates strong possibilities of chemisorption. The measured equilibrium and kinetic data indicate the fitness of Freundlich isotherm and pseudo-second-order model, respectively.

Keywords: Activated carbon; Electroless plating solution; Adsorption; Ni(II) removal

1. Introduction

Heavy metal removal from wastewater streams is an important area of research. Typical permissible limit for Ni in wastewater is about 1–3 mg/L [1]. The various technologies that have been investigated in order to bring down Ni(II) concentrations to permissible levels are adsorption, chemical precipitation, electrochemical reduction, sulphide precipitation, cementation, ion exchange, reverse osmosis, electro dialysis, solvent extraction and evaporation [1,2]. Among these alternative technologies, adsorption is one of the most viable and industrially feasible due to its low cost, design simplicity and wide range of adsorbents available.

The adsorbents that have been studied for wastewater treatment and heavy metal removal include pineapple stem- and bamboo stem-activated carbon [3], meranti sawdust [4], tea waste [5], brown algae [6], chitosan [7] and carbohydrate biopolymer

---

*Corresponding author.

[8]. In most cases, experimental investigations were carried out using aqueous solutions or wastewater streams [2,3,9–15]. Very few investigations addressed Ni(II) adsorption from electroplating solutions [16–20]. Thereby, they address the specific role of solution complexity in influencing heavy metal adsorption characteristics. Further details with respect to these literatures are presented as follows:

Low et al. [16] carried out a comparative study on the adsorption characteristics of acid-treated banana pith for various heavy metals like Cu, Ni, Pb, Cr and Zn from electroplating waste and synthetic solutions under both batch and continuous flow conditions. The affinity of metal sorption was in the order of Pb(II) > Cu(II) > Ni(II) > Cr(II) > Zn(II). The solution metal concentrations were in the range of 10–78 mg/L. Solution complexity involved the inclusion of other chemicals such as $CuSO_4·5H_2O$ and $Ni(NO_3)_2·6H_2O$. The banana pith adsorbent provided a removal efficiency of 3.90% at pH 1.54 which increased to 80.2% at a pH 4.50 for Cu(II). The removal efficiency for Ni(II) varied from 90.81 to 2.59% for a variation in initial Ni(II) solution concentration from 0.280 to 28 mg/L.

Ajmal et al. [18] studied the adsorption characteristics of orange peel to remove Zn, Ni, Cu, Pb and Cr from electroplating wastewater. The maximum adsorption efficiency obtained was for Ni(II) (97.5%) at an optimum pH of 6. For Cr(VI), lowest removal efficiency was obtained (30%). The Ni(II) adsorption capacity increased from 80 to 158 mg/g with an increase in temperature from 30 to 50˚C to confirm that the adsorption process was endothermic.

Ewecharoen et al. [21] studied the adsorption characteristics of Ni(II) from electroplating rinse water using coir pith and modified coir pith. The Ni(II) concentration in the rinse water was 145 mg/L. For experimental investigations, the pH was varied from 2 to 7 along with an adsorbent dosage variation from 1 to 10% w/v in a 15 mL bottle (about 10–100 mg/L). The optimum parameters obtained for adsorption were as follows: pH range of 4–7, optimum adsorption time of 10 min, adsorbent dosage of 5% w/v (for every 10 mL of Ni(II) rinse water) and a temperature of 30˚C. At equilibrium contact time of 10 min, 88% Ni(II) was adsorbed by 5% w/v of adsorbent. The maximum Ni(II) uptake values were 9.5 and 38.9 mg/g for coir pith and modified coir pith adsorbents, respectively. Elution with sulphuric acid confirmed that this process was chemisorption. The adsorption process fitted well with Langmuir model.

Thus, it is apparent that literature data for Ni(II) adsorption from synthetic and real electroplating wastewaters is limited and so is data for the effects of solution complexity on adsorption characteristics. Hence, further research needs to be carried out to evaluate the specific role of solution complexity on adsorption characteristics. Further, insights are also required for wider solution concentrations (50–500 mg/L) to judge upon the efficacy of the activated carbon adsorbent.

Considering the available state of the art, this work addresses the following issues. Firstly, synthetic electroless plating solutions have been used to study the adsorption characteristics of activated carbon adsorbent for Ni(II) adsorption. Electroless plating solutions are important components in the electroplating industry, with the process being one of the most cost effective methods for Ni deposition on non-conducting surfaces. Till date, about 200–300 international journal publications and about 20–50 US patents exist in the field of nickel electroless plating and associated product development. Taking into consideration all these aspects, a preliminary study of Ni(II) adsorption from electroless plating solutions will be beneficial to provide reference data for further analysis and research incentives in the field of adsorption from electroless plating solutions. The synthetic electroless plating solutions consist of nickel sulphate, trisodium citrate (stabliliser), NaOH and HCl as major constituents. Secondly, for comparison purpose, Ni(II) adsorption characteristics obtained for aqueous solutions in our earlier work was considered by Rajesh et al. [3]. Thereby, based on the comparative assessment, the optimality of adsorption parameters for Ni(II) adsorption from synthetic electroless plating solutions is targeted. In summary, this work intends to provide insights into the role of solution complexity, wider combinations of pH range (2–14), Ni(II) concentration (50–500 mg/L) and adsorbent dosages (0.5–4 g/L) on the Ni(II) adsorption characteristics of activated carbon using synthetic electroless plating solutions. Thereby, the specific novelty of the carried research refers towards the evaluation of trisodium citrate (TSC) and NaOH in influencing the Ni (II) adsorption characteristics of commercial activated carbon adsorbent.

2. Materials and methods

2.1. Materials

Ni(II) ELP solutions in aqueous medium were prepared using Millipore water, nickel sulphate heptahydrate ($NiSO_4·7H_2O$), trisodium citrate (TSC) and NaOH. All the chemicals were procured from Merck India. Additional pH adjustments were carried out using 0.1 M HCl solution. Commercial activated charcoal (AC) (CAS No. 7440-44-0) was purchased from Merck India Limited, Mumbai and was used as the adsorbent.

2.2. Preparation of stock solutions

Ni(II) ELP solution concentration was chosen based on the prior experience in the field of NI(II) ELP process for composite membrane fabrication [22]. Based on the laboratory-formulated Ni(II) synthetic ELP solution composition, it was assumed that during ELP process, 30–60% conversion of 0.08–0.16 M Ni(II) and 20% conversion of TSC occurs during the fabrication of Nickel–ceramic composite membranes [22]. Thereby, the composition of the synthetic Ni(II) ELP solution for the current work was chosen as follows: 0.239–2.39 g/L of $NiSO_4 \cdot 7H_2O$ (equivalent to 50–500 mg/L of Ni(II) solution concentration), 626 g/L of TSC and 4 g/L (0.1 M) of NaOH in aqueous medium.

2.3. Adsorbent characterisations

AC adsorbent characterisation was carried out using the following instruments:

1. Laser particle size analyzer (LPSA): LPSA (Make: M/s Malvern Instruments Ltd) was used to estimate the average size (μm) of particles constituting the adsorbent.
2. Brunauer–Emmett–Teller (BET) instrument: Based on N_2 adsorption, BET instrument (Make: Backman Coulter) was used to determine the specific surface area of the adsorbent.
3. Fourier transform infrared (FTIR) spectroscopy: FTIR instrument (Make: M/s Toshvin Analytical Pvt. Ltd) enables the identification of the various functional groups present in the adsorbent by analysing the peaks corresponding to the frequencies associated to specific functional groups on the adsorbent before and after adsorption. The vibrations in the molecules were measured within the frequency range of 500–4,500 cm^{-1}.

2.4. Batch adsorption experiments

Batch adsorption experiments were conducted using synthetic Ni(II) ELP solutions with a natural pH of 5–6 in the solution concentration range of 50–500 mg/L. For these experiments, 50 mL ELP solutions were transferred to 250-mL conical flasks to which commercial AC adsorbent was added to achieve an adsorbent dosage range of 0.5–4 g/L. Further variation in the pH of the solutions was achieved in the range of 2–14 using 0.1 M NaOH and HCl solutions. Batch adsorption was facilitated in an orbital shaker at a rotational speed of 200 rpm. For preliminary adsorption experiments, the sorption time was varied from 30 to 300 min, from where equilibrium time was evaluated. All other experiments were conducted with the evaluated equilibrium time. After batch adsorption process was complete, Whatman 40 filter paper was used to filter the adsorbent and the adsorbate. Eventually, the feed and spent adsorbate samples were analysed using atomic absorption spectrophotometer (Make: Spectra AA220FS), at a wavelength of 232 nm. Based on the calibration chart prepared prior using precise concentrations of synthetic ELP solutions, the Ni(II) solution concentrations in the feed and effluent samples were evaluated. Using the adsorption process parameters and variables, percentage removal and capacity (metal uptake) values were evaluated using the following expressions:

$$\% \text{ Adsorption or } \% \text{ Removal} = \frac{C_e - C_o}{C_o} \times 100 \tag{1}$$

$$\text{Metal Uptake } (q_e,\ \text{mg/g}) = V \times \frac{(C_o - C_e)}{W} \tag{2}$$

where C_o is the initial concentration of Ni(II) in aqueous solution (mg/l), C_e is the equilibrium adsorption concentration of Ni(II) (mg/l), W is the adsorbent dosage (g), V is the volume of aqueous solution (mL) and q_e is the mass of solute adsorbed per mass of adsorbent at equilibrium (mg/g).

Each experiment was conducted at least three times and the average value was reported in the manuscript. Based on the measurements, the maximum and minimum error in the estimation of metal uptake is ±2.36 and ±0.92%, respectively. Similarly, the maximum and minimum error in the estimated values of removal efficiency is about ±0.58 and ±0.35%, respectively.

Further, the point of zero charge (PZC) was also evaluated for the commercial AC. The point of charge (PZC) of a solution containing the adsorbent is defined as the pH at which the observed charge on the adsorbent's surface is zero. It is measured by the pH drift method. Thus, when an adsorbent is in a solution whose pH is less than its PZC, protonation of the functional groups occurs on the adsorbents surface due to which the adsorbent becomes positively charged and adsorption is thereby not favoured for the positively charged metal ions from the solution [23]. Hence, the optimum pH for metal adsorption is generally slightly higher than the PZC of the adsorbent.

The PZC of AC adsorbent was calculated by preparing a 0.05 M solution of $CaCl_2$. After heating the solution to a higher temperature, 50 mL of the solution was mixed with the optimum adsorbent dosage in 250-mL flasks. Subsequently, the pH of the solution was set between 2 and 12 using 0.1 M HCl and NaOH. Eventually, the adsorption flasks were kept in the orbital shaker for 24 h after which their pH was again measured. Using the obtained data, a plot was prepared between the initial and final pH values. To this plot, a 45° line was drawn from the origin. The ordinate of the point where two curves intersect refers to the PZC of the adsorbent.

2.5. Modelling

The data required for designing sorption systems are obtained from analysing the equilibrium sorption data. The process of adsorption completely depends on the interaction between the adsorbate and adsorbent. This interaction could be due to chemical bonds, hydrogen bonds or van der Waals forces of attraction. The existing adsorption isotherms evaluate the relationship between the capacity (weight of adsorbate adsorbed by unit weight of adsorbent) and the amount of solute remaining in the solution at equilibrium.

2.5.1. Fitness of equilibrium isotherm models

The most frequently used isotherm models are the Langmuir and Freundlich models. Both these models can be applicable to adsorption equilibrium depending on whether the adsorption is in monolayer or multilayer, respectively.

The Langmuir equilibrium isotherm model assumes a monolayer coverage on a homogenous adsorbent surface, with no interaction between the adsorbed ions. Thereby, the model is generally represented as [24–26]:

$$\frac{C_e}{q_e} = \frac{1}{bq_{\max}} + \frac{1}{q_{\max}} C_e \tag{3}$$

where C_e is the equilibrium adsorption concentration of Ni(II) (mg/l), q_e is the mass of solute adsorbed per mass of adsorbent at equilibrium (mg/g), $q_{\max}$ is the Langmuir monolayer capacity (mg/g) and b is the Langmuir equilibrium constant.

The favourability of an adsorbent towards an adsorbate is confirmed by evaluating the separation factor (K_R) as a function of the Langmuir isotherm model parameters using the following expression:

$$K_R = \frac{1}{1 + bC_o} \tag{4}$$

where C_o is the initial concentration of Ni(II) in aqueous solution (mg/L). Typically, adsorption is regarded to be favourable for systems where K_R values are in the range of 0–1.

The Freundlich equilibrium isotherm model assumes an exponential distribution of active centres which possess characteristics of heterogeneous surface and infinite surface coverage. The Freundlich isotherm model is commonly represented as [25]:

$$\log(q_e) = \log(K_F) + m \log(C_e) \tag{5}$$

where K_F is the Freundlich isotherm coefficient and m is the amount of adsorbent taken (mg/L).

The fitness of either of the above models was confirmed by evaluating the coefficient of correlation (R^2) value for the graphs prepared to represent the models using presented expressions.

2.5.2. Fitness of kinetic models

In general, the kinetics of an adsorption process are represented using either pseudo-first-order or pseudo-second-order models. The Lagergren equation [27] is used to represent the pseudo-first-order kinetics and is expressed as follows:

$$\log(q_e - q_t) = \log(q_e) - \frac{k_1}{2.303} t \tag{6}$$

where q_e is the mass of solute adsorbed per mass of adsorbent at equilibrium (mg/g), q_t is the mass of solute adsorbed per mass of adsorbent at "t" min, (mg/g), t is the agitation time (min) and k_1 is the first-order rate constant (min^{-1}).

The adsorption in pseudo-second-order reaction is dependent upon the valence forces of the adsorbent on the adsorbate and adsorption occurs because of the exchange of electrons between these two. The removal of the solute from the solution is hypothesised due to physico-chemical reactions. The pseudo-second-order model is expressed as follows [28]:

$$\frac{t}{q} = \frac{1}{k_2 {q_e}^2} + \frac{1}{q_e} t \tag{7}$$

where q_e is the mass of solute adsorbed per mass of adsorbent at equilibrium (mg/g), t is the agitation time (min) and k_2 is the pseudo-second-order rate constant (g mg^{-1} min^{-1}).

The fitness of either of the models towards experimentally obtained adsorption kinetics data was evaluated using a graphical method that represented the above presented model expressions. Eventually, the plot that gave the highest value of coefficient of correlation (R^2) and the lowest values of various errors, minimal ($Er_{\min}$), maximum ($Er_{\max}$), average (Er_{avg}) and RMS error (RMSE) was regarded to be the best fit model. These errors were evaluated using the expressions:

$$Er_i = \frac{|C_i^{\exp} - C_i^{\text{model}}|}{C_i^{\exp}} \times 100 \tag{8}$$

$$Er_{\max} = \text{Max}(Er_i)$$

$$Er_{\min} = \text{Min}(Er_i)$$

$$Er_{\text{avg}} = \frac{\sum_{i=1}^{n} Er_i}{n} \tag{9}$$

$$\text{RMSE} = \frac{\sqrt{\sum_{i=1}^{n} Er_i^2}}{n} \tag{10}$$

where Er is the error function, i is the index for batch adsorption experiment corresponding to specific initial solution concentration of Ni(II), n is the total number of batch adsorption experiments carried out with variant concentration, $Er_{\max}$ is the error maximum, $Er_{\min}$ is the error minimum, Er_{avg} is the average error and Er_{rms} is the root mean square error.

3. Results and discussion

3.1. Surface characterisation by FTIR, BET and LPSA analysis

Fig. 1a shows the FTIR spectral patterns for the commercial AC adsorbent before and after Ni(II) adsorption. It has been analysed that before adsorption, specific peaks corresponding to wave numbers of 3,722, 1,703.14, 1,521.83, 1,342.45, 964.408, and 667.37 cm^{-1} indicate the presence of NH, C=C, OH, CO, C–Cl or C–Br functional groups, respectively. However, after Ni(II) adsorption, the corresponding peak variations were obtained at wave numbers of 3,743.83, 2,395.58, 1,795.722, 1,334.24, 923.90, 837.10, and 611 cm^{-1}. This confirmed that Ni(II) adhesion/bonding occurred to the above-mentioned functional groups as follows: the lone pair of electrons present on nitrogen of NH group attracts the Ni(II) positively charged ions, thus causing them to get adsorbed on the AC adsorbent. The same explanation can be extended to the OH and CO bonds, in which the oxygen atom has two lone pairs of electrons. In addition to this, the partial negative charge present on oxygen of the C=O bond due to shifting of the double bond further strengthens its ability to attract Ni(II). Chlorine and bromine, being extremely electronegative atoms, are able to attract and adsorb Ni(II) ions onto the AC surface. Thus, the FTIR analysis shows that there are stronger possibilities of chemisorption in the batch adsorption process.

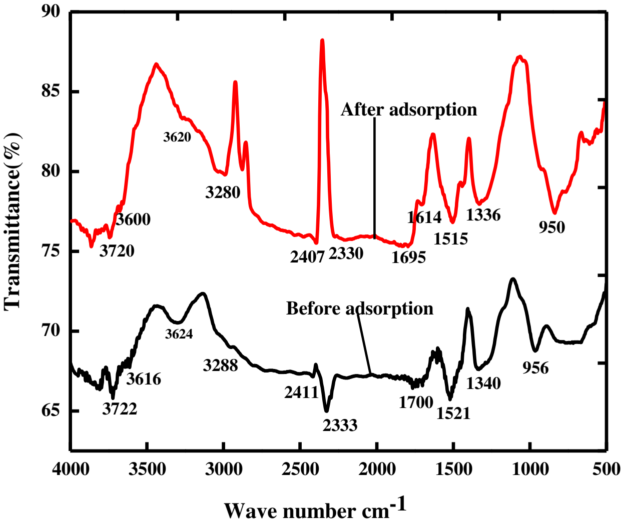

Fig. 1a. FTIR spectral patterns of commercial AC before and after Ni(II) adsorption using synthetic ELP solutions.

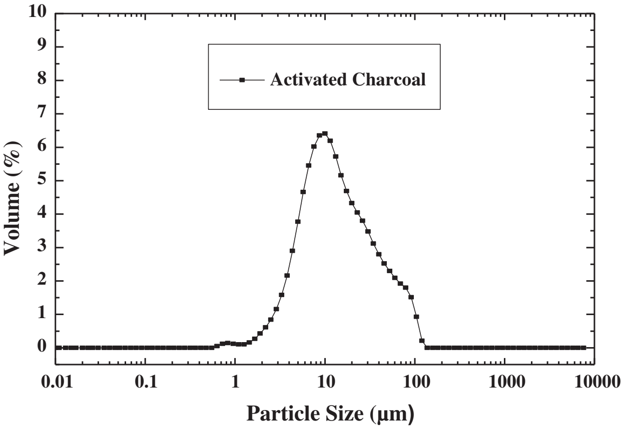

Fig. 1b. Particle size distribution of commercial AC.

The particle size distribution curve obtained with LPSA (Make: Malvern, Model: AWN 2000), operated with the normal operating conditions (Dispersion type: Wet; maximum particle size 1,000–1,500 μm), is presented in Fig. 1b. Based on the obtained particle size distribution curve, the average particle size is evaluated as 25.7 μm. This indicates small size of the adsorbent particles and their favourability towards better adsorption.

The average surface area and pore size of the AC adsorbent was determined using BET surface area analyzer that was operated at 77 K using liquid N_2 after degassing at 200˚C in vacuum for 60 min. The BET surface area of the adsorbent is 1,057.7 m^2/g.

3.2. Effect of adsorption parameters

3.2.1. Contact time

Fig. 2(a) refers to the variation in percentage removal with variation in contact time for the chosen system of adsorbent–adsorbate. For the reported data, other adsorption process parameters refer to 50-mg/L Ni(II) solution concentration, 1-mg/mL adsorbent dosage and pH of 12. It can be observed in the figure that, with an increase in contact time from 30 to 180 min, the percentage removal increased from 0.12 to 5.954% and capacity varied from 0.06 to 2.977 mg/g, respectively. While the percentage removal and capacity varied significantly up to a time period of 120 min, an insignificant enhancement was observed in these parametric profiles for a further enhancement in time period from 120 to 180 min. Thereby, the optimal adsorption time was evaluated as 120 min., where the metal adsorption and capacity was 5.7% and 2.85 mg/g, respectively. The enhancement in the adsorption rate with increasing adsorption time was due to the availability of free sites which reduced significantly after saturation. The observed enhancement in both metal uptake and % removal are in accordance with the trends presented in the relevant literature [3,12,14,16].

3.2.2. pH

Fig. 2(b) presents the effect of pH on the variation in %removal and metal uptake. For this case, other adsorption process parameters refer to 50-mg/L Ni(II) solution concentration, 1-mg/ml adsorbent dosage and equilibrium contact time of 120 min. It can be observed that adsorption process variables are strongly influenced by the solution pH. The optimal pH corresponds to 10.55 where the % removal and capacity have been evaluated as 17.58% and 8.79 mg/g, respectively. Incidentally, the PZC value for the adsorbent was evaluated to be 10.23, which is slightly lower than the optimal pH. The observed trends of the pH effect are in accordance with the relevant literature [17].

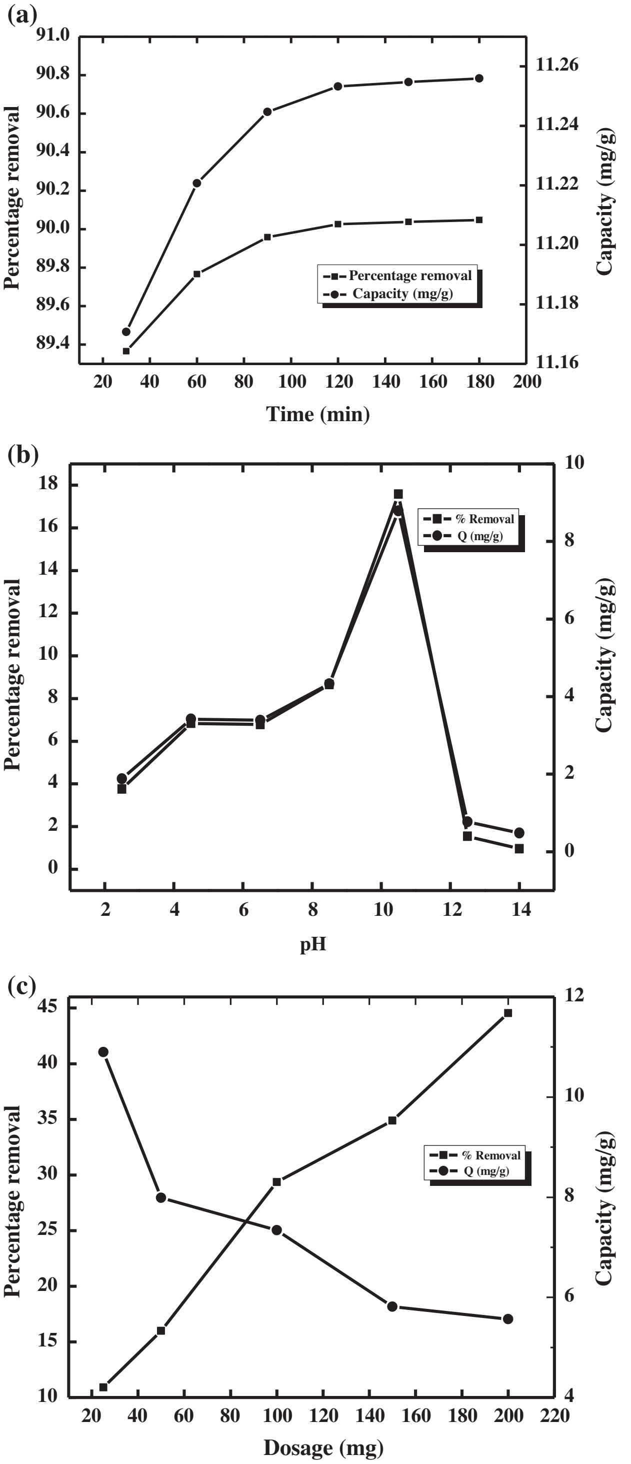

Fig. 2. Effect of batch adsorption process parameters on % removal and metal uptake from Ni(II) containing synthetic ELP solutions: (a) contact time (min); (b) pH and (c) dosage (mg).

3.2.3. Adsorbent dosage

Fig. 2(c) shows the effect of adsorbent dosage on Ni(II) adsorption characteristics of synthetic ELP solutions. For this case, other adsorption process parameters refer to an optimal pH of 10.55, optimal equilibrium time of 120 min and Ni(II) solution concentration of 50 mg/L. It can be observed that, for a variation in adsorbent dosage from 0.5 to 4 g/L, the % removal and capacity values varied from 10.9 to 44.54% and 10.89 to 5.75 mg/g, respectively. The enhancement in the removal values is due to the availability of larger number of active sites at higher adsorbent dosage. Since a plateau was observed at 4 g/L adsorbent dosage value, the same has been referred to as the optimal adsorbent dosage. The decrease in the uptake values can also be attributed to the increase in the number of active sites as the metal ions have greater number of sites to get adsorbed onto. Observed trends in adsorption process characteristics with dosage variation are in agreement with those reported in the literature [3,12,14,16].

3.2.4. Ni solution concentration

The primary objective of this article is to evaluate upon the role of solution complexity in influencing Ni(II) adsorption characteristics. The effect of Ni(II) solution concentration on the adsorption characteristics with synthetic ELP solutions is presented in Fig. 3(a) and (b). For comparative purpose, the data obtained from our earlier work using bamboo stem-activated carbon adsorbent (surface area = 111 m^2/g) and Ni(II) aqueous solutions (solution concentration of about 50–300 mg/L) has also been presented in respective plots. For these experiments, the fixed choice of other adsorption process parameters refers to a pH of 10.55, adsorbent dosage of 4 g/L and equilibrium contact time of 200 min.

It can be observed that Ni(II) solution concentration significantly influenced adsorption characteristics. For a variation in initial solution concentration from 50 to 500 mg/L, the % removal and metal uptake values varied from 44.54 to 5.56% and 14.2 to 17.75 mg/g, respectively. Corresponding trends in the % removal and capacity values for BSAC aqueous solutions case refer to a variation of about 92.74–61.23% and 16.84–91.59 mg/g, respectively. Thus, it is apparent that significantly lower trends for both % removal and metal uptake were obtained for the synthetic ELP solutions in comparison with aqueous solutions. This is attributed to the presence of trisodium citrate in the ELP solutions which strongly inhibited Ni(II) adsorption to the AC adsorbent surface. The strong inhibition due to the TSC is probably due to the competitive adsorption of TSC to the adsorbent surface. Thus, it is very important to carry out realistic adsorption experiments during laboratory experimental investigations for heavy metal adsorption.

Table 1 presents a comparative summary of Ni(II) adsorption data provided in the literature for aqueous and electroplating solutions. It can be observed that the

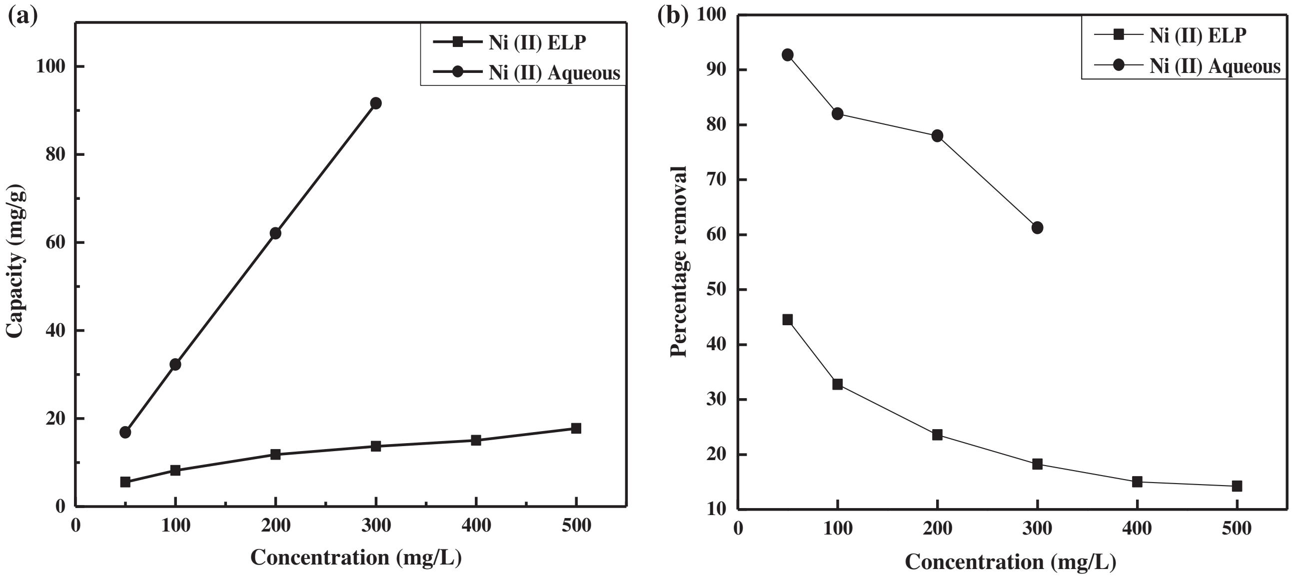

Fig. 3. Effect of Ni(II) solution concentration on the adsorption characteristics: (a) capacity and (b) % removal.

Table 1
Comparative summary of Ni(II) adsorption characteristics of various feed solutions

Adsorbent	Type of solution	Range of solution concentration (mg/L)	Maximum metal uptake (mg/g)	Range of percentage adsorption (%)	Refs.
Bamboo stem-activated carbon	Aqueous	50–300	98.07	92.74–65.38	[3]
Pineapple stem-activated carbon	Aqueous	50–300	29.1	85.24–58.2	[3]
Raw charcoal of *Melocanna baccifera*	Aqueous	30–70	–	18.5–15.7	[2]
Activated carbon	Electroplating	2.93–293.4	8.58	90.81–2.59	[16]
Commercial AC	Electroless plating	50–500	17.75	44.54–5.56	Present work

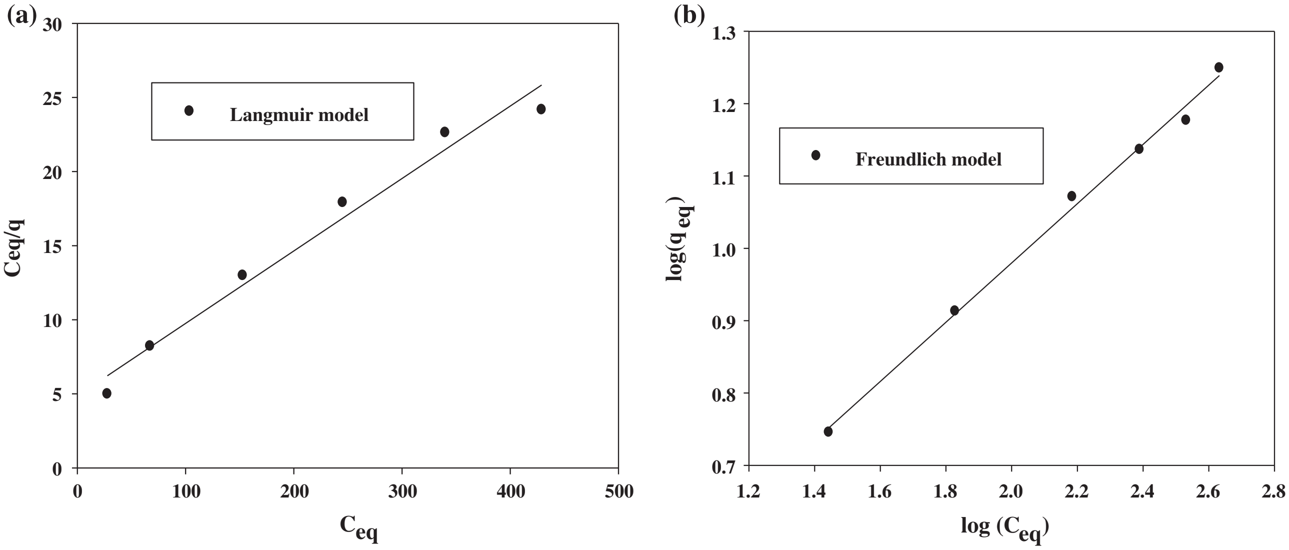

Fig. 4. Graphical fitness plots for (a) Langmuir and (b) Freundlich isotherm models to represent measured Ni(II) equilibrium adsorption data from synthetic ELP solutions.

% removal is strongly influenced with solution complexity. For electroplating solutions, % removal has been as low as 2.59% at higher Ni(II) solution concentration which is in agreement with the % removal obtained in this work for the higher Ni(II) solution concentration. This was not the case for the adsorption data reported for Ni(II) aqueous solutions where higher % removal values (58–65%) were obtained at higher Ni(II) solution concentrations. All in all, the evaluated adsorption characteristics are strongly indicative towards the need for further complexities in the case studies targeted in laboratory experimental investigations.

The solution complexity in this work refers to the combined effect of trisodium citrate and NaOH in compared to the aqueous medium. Since the adsorption characteristics for the former case were significantly lower than those obtained for the latter case, it has been opined that solution complexity strongly influences the adsorption characteristics. Further insights into the mechanism could not be addressed as the experimental investigations did not elaborate upon the effect of each of the chemicals (i.e. NaOH and trisodium citrate). It is hypothesised that the solution containing TSC and Na^+ might favour significant adsorption of Na^+ on the active sites due to which reason Ni(II) could not be adsorbed significantly. Thereby, further insights can be gained in the mechanism by carrying out additional adsorption studies with more variations in solution palette, which are anticipated in the near future.

Table 2
Various parameters obtained for the fitness of Langmuir and Freundlich equilibrium isotherm models to measured Ni(II) adsorption data

			Error			$q_{\max}$ (mg/g)		
Model	R^2	RMS	Avg	Max	Min	Exp	Cal	Model Parameters
Langmuir	0.9762	11.182	8.06	24.84	0.78	17.75	20.449	$b = 4.205$ $K_R = 0.0085$
Freundlich	0.9952	1.067	0.923	1.748	0.250	17.75	–	$K_F = 1.448$ $n = 2.442$

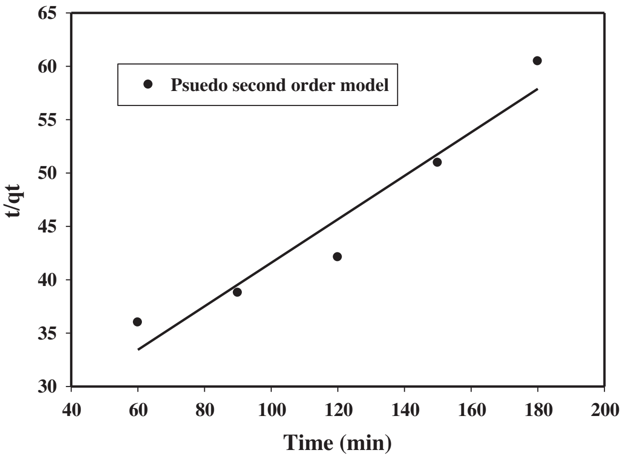

Fig. 5. Fitness plot for pseudo-second-order model to represent Ni(II) adsorption kinetics data.

3.3. Fitness of isotherm models

Fig. 4(a) and (b), respectively, present the graphical fitness plots for Langmuir and Freundlich isotherm models for measured Ni(II) adsorption data with synthetic ELP solutions. Table 2 presents the corresponding summary of coefficient of correlation (R^2), various errors and model parameters for both the models. For the Langmuir isotherm model, the R^2 value is about 0.9762. Corresponding RMS, average, maximum and minimum error values were evaluated as 11.182, 125.043, 617.426, and 0.610, respectively. K_R value was evaluated to be within the range of 0–1, which confirmed the utility of the adsorbent towards favourable adsorption. For the Freundlich isotherm model, the R^2 value was evaluated as 0.9952. Corresponding RMS, average, maximum and minimum error values were evaluated as 1.067, 1.139, 3.056, and 0.062, respectively. Thus, based on the obtained fitness parameter values, it can be confirmed that Freundlich isotherm represents the measured Ni(II) adsorption characteristics with synthetic ELP solutions and commercial AC adsorbent, thereby indicating that the adsorption process is heterogeneous in nature.

3.4. Fitness of kinetic models

A negative slope was obtained for the graphical plot associated to represent the pseudo-first-order kinetic model for the measured adsorption kinetics data. Hence, pseudo-first-order model was inferred to be not applicable for the measured data. Fig. 5 presents the graphical fitness plot for pseudo-second-order model. Corresponding coefficient of correlation, error values and model parameters are presented in Table 3. It was evaluated that the pseudo-second-order model had an R^2, RMS, average, minimum and maximum error values of 0.932, 17.98, 16.6, 24.37, and 8.14%, respectively. Significant error values for kinetic data indicate the complexity associated with competitive adsorption of TSC and Ni(II) to the adsorbent surface. Also, k_2 was evaluated as 1.95×10^{-3} which confirmed that the rate-limiting step in the adsorption kinetics refer to chemisorptive surface adsorption.

Table 3
Various parameters obtained during fitness studies conducted for pseudo-second-order kinetic model

	q_e (mg/g)					Error		
C_o (mg/l)	Exp	Cal	R^2	$k_2 \times 10^{-3}$	RMS	Average	Max	Min
50	1.67	0.047	0.932	1.95	17.989	16.63	24.37	8.14

4. Conclusion

The reported experimental investigations for synthetic ELP solutions and commercial AC adsorbent provided significant insights. Firstly, for synthetic ELP solutions, optimal adsorption process parameters for commercial AC adsorbent refer to an optimal combination of pH, contact time, adsorbent dosage and Ni (II) solution concentration as 10.55, 120 min, 4 g/L and 50 mg/L, respectively where maximum metal uptake and % removal can be obtained. Secondly, significant reductions in metal uptake and % removal have been observed for synthetic ELP solutions in comparison with aqueous solutions. Thus, solution complexity and precisely TSC contributed significantly towards the inhibition of Ni(II) adsorption on to the adsorbent surface. Henceforth, realistic experimental investigations need to be carried out in various approaches adopted for heavy metal adsorption. Thereby, the recovery of Ni(II) from synthetic ELP solutions containing TSC is apparent to be a highly challenging problem from the perspective of adsorption-based process technology. Thirdly, the fitness of Freundlich isotherm and pseudo-second-order kinetic models indicated strongly the possibilities of irreversible chemisorption which pose further challenges towards the regeneration of the commercial AC adsorbent. These insights are anticipated to serve as useful reference data to further research opportunities in the field of Ni(II) recovery and reuse from electroless plating solutions. The research work inferred that significant challenges exist towards low-cost Ni(II) removal from electroless plating solutions consisting trisodium citrate stabiliser in basic medium.

References

[1] P.S. Kumar, K. Kirthika, Equilibrium and kinetic study of adsorption of nickel from aqueous solution onto bael tree leaf powder, J. Eng. Sci. Technol. 4 (2009) 351–363.

[2] H. Lalhruaitluanga, M.N.V. Prasad, K. Radha, Potential of chemically activated and raw charcoals of *Melocanna baccifera* for removal of Ni(II) and Zn(II) from aqueous solutions, Desalination 271 (2011) 301–308.

[3] Y. Rajesh, M. Pujari, R. Uppaluri, Equilibrium and kinetic studies of Ni(II) adsorption using pineapple and bamboo stem based adsorbents, Sep. Sci. Technol. 49 (2014) 533–544.

[4] A. Ahmad, M. Rafatullah, O. Sulaiman, M.H. Ibrahim, Y.Y. Chii, B.M. Siddique, Removal of Cu(II) and Pb(II) ions from aqueous solutions by adsorption on sawdust of Meranti wood, Desalination 247 (2009) 636–646.

[5] P. Panneerselvam, N. Morad, K.A. Tan, Magnetic nanoparticle (Fe_3O_4) impregnated onto tea waste for the removal of nickel(II) from aqueous solution, J. Hazard. Mater. 186 (2011) 160–168.

[6] M.M. Montazer-Rahmati, P. Rabbani, A. Abdolali, A.R. Keshtkar, Kinetics and equilibrium studies on biosorption of cadmium, lead, and nickel ions from aqueous solutions by intact and chemically modified brown algae, J. Hazard. Mater. 185 (2011) 401–407.

[7] K.J. Hsien, C.M. Futalan, W.C. Tsai, C.C. Kan, C.S. Kung, Y.H. Shen, M.W. Wan, Adsorption characteristics of copper(II) onto non-crosslinked and crosslinked chitosan immobilized on sand, Desalin. Water Treat. 51 (2013) 5574–5582.

[8] V.T.P. Vinod, R.B. Sashidhar, B. Sreedhar, Biosorption of nickel and total chromium from aqueous solution by gum kondagogu (*Cochlospermum gossypium*): A carbohydrate biopolymer, J. Hazard. Mater. 178 (2010) 851–860.

[9] L.J. Yu, S.S. Shukla, K.L. Dorris, A. Shukla, J.L. Margrave, Adsorption of chromium from aqueous solutions by maple sawdust, J. Hazard. Mater. 100 (2003) 53–63.

[10] P.M. Choksi, V.Y. Joshi, Adsorption kinetic study for the removal of nickel(II) and aluminum(III) from an aqueous solution by natural adsorbents, Desalination 208 (2007) 216–231.

[11] U.K. Garg, M.P. Kaur, V.K. Garg, D. Sud, Removal of nickel(II) from aqueous solution by adsorption on agricultural waste biomass using a response surface methodological approach, Bioresour. Technol. 99 (2008) 1325–1331.

[12] M.H. Helen Kalavathy, L.R. Miranda, *Moringa oleifera*—A solid phase extractant for the removal of copper, nickel and zinc from aqueous solutions, Chem. Eng. J. 158 (2010) 188–199.

[13] A.K. Yadav, N. Kumar, T.R. Sreekrishnan, S. Satya, N.R. Bishnoi, Removal of chromium and nickel from aqueous solution in constructed wetland: Mass balance, adsorption–desorption and FTIR study, Chem. Eng. J. 160 (2010) 122–128.

[14] S. Malamis, E. Katsou, A review on zinc and nickel adsorption on natural and modified zeolite, bentonite and vermiculite: Examination of process parameters, kinetics and isotherms, J. Hazard. Mater. 252–253 (2013) 428–461.

[15] E. Sočo, J. Kalembkiewicz, Adsorption of nickel(II) and copper(II) ions from aqueous solution by coal fly ash, J. Environ. Chem. Eng. 1 (2013) 581–588.

[16] K.S. Low, C.K. Lee, A.C. Leo, Removal of metals from electroplating wastes using banana pith, Bioresour. Technol. 51 (1995) 227–231.

[17] J. Ruey-Shin, K. Hsiang-Chien, W. Chen, Column removal of Ni(II) from synthetic electroplating waste water using a strong-acid resin, Sep. Purif. Technol. 49 (2006) 36–42.

[18] M. Ajmal, R.A.K. Rao, R. Ahmad, J. Ahmad, Adsorption studies on *Citrus reticulata* (fruit peel of orange): Removal and recovery of Ni(II) from electroplating wastewater, J. Hazard. Mater. 79 (2000) 117–131.

[19] F.V. Pereira, L.V.A. Gurgel, L.F. Gil, Removal of Zn^{2+} from aqueous single metal solutions and electroplating wastewater with wood sawdust and sugarcane bagasse modified with EDTA dianhydride (EDTAD), J. Hazard. Mater. 176 (2010) 856–863.

[20] N.M. Salem, A.M. Awwad, Biosorption of Ni(II) from electroplating wastewater by modified (*Eriobotrya japonica*) loquat bark, J. Saudi Chem. Soc. 18 (2014) 379–386.

[21] A. Ewecharoen, P. Thiravetyan, W. Nakbanpote, Comparison of nickel adsorption from electroplating rinse water by coir pith and modified coir pith, Chem. Eng. J. 137 (2008) 181–188.
[22] A. Agarwal, M. Pujari, R. Uppaluri, A. Verma, Optimal electroless plating rate enhancement techniques for the fabrication of low cost dense nickel/ceramic composite membranes, Ceram. Int. 40 (2014) 691–697.
[23] P. Suksabye, P. Thiravetyan, W. Nakbanpote, S. Chayabutra, Chromium removal from electroplating wastewater by coir pith, J. Hazard. Mater. 141 (2007) 637–644.
[24] M. Alhawas, M. Alwabel, A. Ghoneim, A. Alfarraj, A. Sallam, Removal of nickel from aqueous solution by low-cost clay adsorbents, Int. Acad. Ecol. Environ. Sci. 3(2) (2013) 160–169.
[25] A. Radenovic, J. Malina, A. Strkalj, Removal of Ni(II) from aqueous solution by low-cost adsorbents, Holist. Approach Environ. 1 (2011) 109–120.
[26] U. Singh, R.K. Kaushal, Treatment of waste water with low cost adsorbent: A review, VSRD Int. J. Tech. Non-Tech. Res. 4(13) (2013) 33–42.
[27] Y.S. Ho, G. McKay, Pseudo-second order model for sorption processes, Process Biochem. 34 (1999) 451–465.
[28] Y.S. Ho, C.T. Huang, H.W. Huang, Equilibrium sorption isotherm for metal ions on tree fern, Process Biochem. 37 (2002) 1421–1430.